Face Mask Detection Based on GLCM Feature Extraction and Image Classification using Machine Learning Techniques To Counter Airborne Diseases

Azlou Jamal*, Mehdi Khamir**, Anouar Imel**, Ilyas Raij**, Labbane Abdellah**,El Barnoussi Fatima Ezzahra**
*School of Artificial Intelligence, Nanjing university of Information Science and Technology
Email: jamal.azlou0@gmail.com
**School of Artificial Intelligence, Nanjing university of Information Science and Technology
(mehdi_khamir@um5.ac.ma, Anouarimel21@gmail.com, fatima.ilbarnoussi@gmail.com)
**School of Computer Science, Nanjing university of Information Science and Technology
(Ilyas-raij@outlook.fr, Labbane.abdellah@gmail.com)

--*************************----------------------------------

Abstract—Airborne diseases have immensely affected the world from the 13th century's black death to the 21st century's COVID-19 claiming millions of lives. Preventive measures were put in place to counter the spread of airborne diseases. Face mask use has been proven effective and hence advocated by the WHO (World Health Organization). Extracted GLCM Texture features are used for face mask detection using LightGBM. 3833 RGB images, including 1915 masked and 1918 unmasked images sampled from RMFD and SMFD image collection, plus several personally taken images using a webcam are used to train the proposed network. The proposed approach has proved effective, with 87% accuracy in detecting masked individuals.

Keywords — **face mask, airborne diseases, LightGBM, GLCM, COVID-19, SMFD, RMFD**

--*************************----------------------------------

I. INTRODUCTION

Airborne diseases are responsible for various epidemics that have taken a toll on humankind, from the black death in the 1300s, claiming an estimated 75-200 million lives to COVID-19 desolating the globe claiming 6,152,095 lives, causing 489777062 cases as of April 4, 2022, according to WHO.COVID- 19 as a case, tremendous measures had to be taken, including lockdown(Local and Nationwide), social distancing, compulsory use of face masks, and hand hygiene, as primary preventive to counter the spread of SARS-Cov-2. Numerous studies have proven Face mask usage as a pillar to counter Airborne diseases, Wu Lien Teh's efforts to contain the Manchurian Epidemic of 1910 have been lauded as “a milestone in the systematic practice of epidemiological principles in disease control” [1] in which Wu refers to the fabric mask as “the principal means of personal protection.” Wu pointed out that the airborne transmission of diseases has been recognized since the 13th century, despite the fact that he created the cloth mask that was widely used worldwide in the early twentieth century. Since the 14th century, people have been advised to wear face coverings to protect themselves from respiratory pandemics [2]. A study carried out in Beijing ménages envisioned plummeting secondary transmission of SARS-CoV-2 by means of face mask usage [3]. Face masks have proved to be 79 percent efficient in avoiding diffusion when used worn by all members of the ménage before symptoms appeared. To assess the association between mask use and SARS-CoV-2 dissemination, Leffler et al.

[4] employed a multiple regression technique that included a variety of policy interventions as well as nation and population factors. They discovered that dissemination was 7.5 times higher in nations without a mask mandate or ubiquitous mask wear, a finding similar to one found in a smaller study [5].

II. PAGE LAYOUT

All mentioned studies and more supported the face mandate to be put in place. This created an opportunity for developers and researchers to design systems to assist the compliance of the set rules to curb COVID-19.

M. M. Rahman et al. [6] employed CNN to extract, and classify features following preprocessing the data. The trained algorithm has a 98.7% accuracy rate in detecting individuals without face masks and alerting authorities to help limit the diffusion of COVID-19. By employing pre- trained CNNs to extract candidate facial regions and express the regions with high-dimensional descriptors, Ge et al. [7] suggested an LLE-CNN to recognize masked faces. To satisfy lower computational requirements for embedded devices, Fan et al. [8] suggested a deep learning-based single-shot lightweight face mask detector. They developed a well-functioning SL-FMDet thanks to its reduced hardware needs.

M.S. Ejaz et al. [9] employed the Viola-Jones methodology to implement PCA for masked and non-masked facial image recognition, and face components. Face recognition is performed simultaneously using PCA to derive Eigenface and the closest neighbor (NN) classifier distance.

M. Loey et al. demonstrated the performance of various machine learning methods in recognizing face masks

and numerous applications in their study [10]. ResNet50 is applied to extract features from three used datasets in this work. For the classification purpose, employed are decision tree algorithm, support vector machine, and ensemble algorithms, resulting in excellent detection accuracy on every used dataset.

Retina Facemask is a paradigm for identifying the face mask that combines it with a bridge entity removal approach, according to Jiang et al. [11]. A single-stage detector based on a feature pyramid network is included in the proposed model, which achieves somewhat greater precision and recall than the baseline result. They employed a learning algorithm [12], as well as deep learning [13-16] technique, to solve the shortage of datasets.

Since the publication of texture features utilizing GLCM by K. Haralick et al. [17] in 1973, texture features have been widely popular in image classification applications, particularly in the biomedical field. Using GLCM, H. Chai et al. [18] proposed a methodology to assess the femur's long bone fracture performance in 2011. J. Ding et al. [19] 2017 used a variety of ML algorithms, like SVM, K-mean clustering, and deep learning tactics, obtaining seventeen GLCM features for Massive Scale Image Data validation and verification.

With fitness function plus diagonal class entropy on raw satellite images, Z. Xing et al. [20] proposed the affected salp swarm technique for enhancing GLCM.

The use of GLCM to extract texture features seemed promising to differentiate a masked individual from an unmasked individual due to the outstanding performance of texture features using GLCM in Image classification tasks and the difference in texture between an unmasked image and its masked counterpart; thus implemented in this study.

III. PAGE STYLE

Using publicly available datasets, the dataset used in this study was constructed with a total of 3833 RGB images, including 1915 masked and 1918 unmasked images sampled from a combination of RMFD [16] a collection of masked face data from throughout the world as well as the Simulated SMFD [17], plus a number of personally taken images using a webcam. The images were split and used for training and testing set to experiment with this study with two classes, respectively.

Figure 1: Dataset samples (a) Masked (b) Unmasked

Preprocessing is required since the images in the collection are not all the same size. All images were resized to 128 ×128 pixels employing Keras' Image Data Generator.

IV. PROPOSED WORK

A. The suggested technique is split into three steps, which are as follows:

B. Preparation of Images

C. Extraction of Features

D. Classification Approach

E. The proposed strategy is depicted in Figure 2 below as a block diagram.

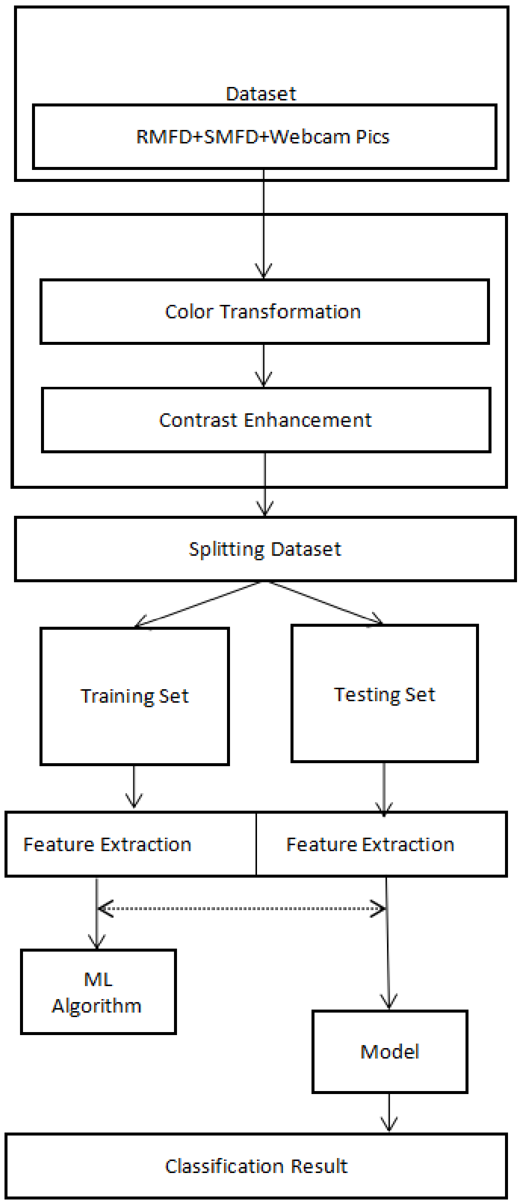

Figure 2: Schematic representation of the suggested strategy

A. Preparation of Images

The main goal of the Image Preparation stage is to apply color transformations (RGB to grey), resize, and improve image contrast, among other things.

 Color transformation: This stage necessitates the conversion of RGB images to grayscale, which can be achieved using a variety of approaches, including the weighted approach, average method, and brightness approach. The luminosity approach was employed in this study, with Red providing 21%, Green providing 72%, which is the most significant in all three hues, and Blue providing 7%.

 Contrast Enhancements: Because some images may be flawed and inadequate in some critical data such as jagged staining and poor resolution, it is necessary to enhance the object in the image, especially for masked cases, so the CLAHE (contrast limited adaptive histogram equalization) technique with clip threshold set to 5 is used. Figure 3 shows the initial image and the improved image, as well as the contrast-enhanced image.

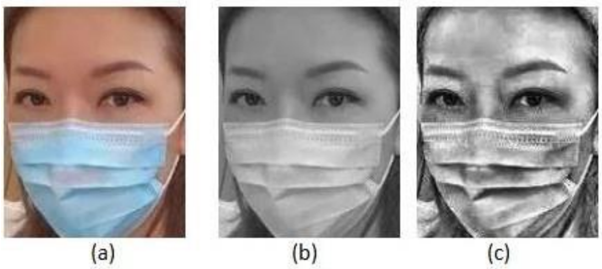

Figure 3: (a) Initial Image, (b) Color transformed

Image, (c) Contrast enhanced image

B. Extraction of Features

features and selection are critical. Images can be classified using a suitable feature extraction method based on distinctive features in this investigation, a GLCM (Gray Level Co-Occurrence Matrix) was utilized. A GLCM is a matrix with the same number of rows and columns as the number of grey levels (G) in the image. R(k, l | v, w) is the frequency with which two pixels separated by a pixel distance (Δv,Δw) appear inside a particular locality, one with intensity I and the other with intensity j, respectively. The second-order statistical probability values for changes between grey levels k and l at a specific angle (θ) and displacement distant correspondingly can be found in the matrix element R(k, l | d, θ)[21].

Let f(a, b) be the intensity at sample a, line b of an A ×

B locality of an input image having G grey levels ranging from

Where

$$T = \frac{1}{(A - \Delta v)(B - \Delta w)}$$

$$O(k, l \mid \Delta v, \Delta w) = \sum_{b=1}^{B-\Delta w} \sum_{A=1}^{A-\Delta v} A$$

And

$$A = \begin{cases} 1 \; if \; (a, b) = k \text{ and } (a + \Delta v, b + \Delta w) = l \\ 0 \; elsewhere \end{cases}$$

The GLCM can be used to extract a variety of texture features.

Taking into account that C is the number of grey levels employed. μ is the average of R's value. Rv and Rw's averages and standard deviations are μv, μw, σv, and σw. Summing the rows of R(k, l) yields the ith item in the marginal-probability matrix:

$R_v(k) = \sum_{j=0}^{C-1} R(k, l)$

$R_w(l) = \sum_{j=0}^{C-1} R(k, l)$

$\mu v = \sum C-1 \; k \sum C-1 \; (k, l) = \sum C-1 \; k Rv \; (k)$

$\mu w = \sum C-1 \; k \sum C-1 \; (k, l) = \sum C-1 \; l Rw(l)$

$\sigma w^2 = \sum^{C-1}(k - \mu v)^2 \sum^{C-1} R(k, l) = \sum^{C-1}(Rw(k) - \mu w(k))^2$

And

R (k)= $\sum C-1 \sum C-1 \; R(k, l) \quad k + l = h$
For h= 0 ,1, …, 2(C-1)

R(v-w) (k)= $\sum C-1 \sum C-1 \; R(k, l) \quad |k - l| = h$
For h= 0, 1, ..., (C-1)

B locality of an input image having G grey levels ranging from 0 to C-1.

The features below were extracted:

- Contrast: The assessment of an image's local intensity fluctuation, pixel intensity and its neighbor over the image. The contrast arises from the difference between the maximum and minimum pixel intensity in an image. The contrast function of an image is illustrated in Equation (4) below:

Contrast =∑C−1 b2 {∑C ∑C R(k, l)}, |k − l| = b
R(i, j | Δx, Δy) = T O(i, j | Δv, Δw) (1)

Angular Second Moment (ASM): demonstrates the image's gray level distribution regularity

ASM= $\sum_{k=0}^{C-1}\sum_{l=0}^{C-1}\{R(k, l)\}2$

ASM ranges from 1/C2 to 1. ASM value of 1 indicates a constant image.

Entropy: the metric by which information content is evaluated. It assesses the degree of unpredictability in the distribution's intensity.

Entropy= $\sum^{C-1}\sum^{C-1}$ R(k, l) × log(R(k, l))

Entropy ranges from 0 to infinity.

Correlation: a metric of gray level linear dependency between pixels at defined distances from one another.

Correlation =$\sum^{C-1}\sum^{C-1}$ {k×l}×R(k,l)−{μv×μw}

Dissimilarity: It estimates the gray level mean difference in the image distribution. A higher number denotes a larger difference in intensity levels between adjacent pixels.

Dissimilarity= $\sum^{C-1}\sum^{C-1}$ |k − l|R(k, l)

Homogeneity: demonstrates the image's resemblance of components (pixels).

Homogeneity=$\sum^{C-1}\sum^{C-1}$ b × R(k, l) where b=|k − l|

Homogeneity ranges from 0 to C-1. A value of 0 indicates a substantial similarity in the image.

Energy: It assesses the degree of textural irregularity in a photograph.

Energy=$\sqrt{ASM}$

V. SIMULATION AND RESULTS

Tensor Flow 2.2 plus Cuda 10.1 are used to implement the suggested methods with an NVidia GeForce RTX 2080 TI GPU and 48 GB RAM PC. A methodology was followed while partitioning the dataset to guarantee that each class was properly represented in the test set and training set. The total number of masked and unmasked instances in the created dataset for this project is shown in Figure 4.

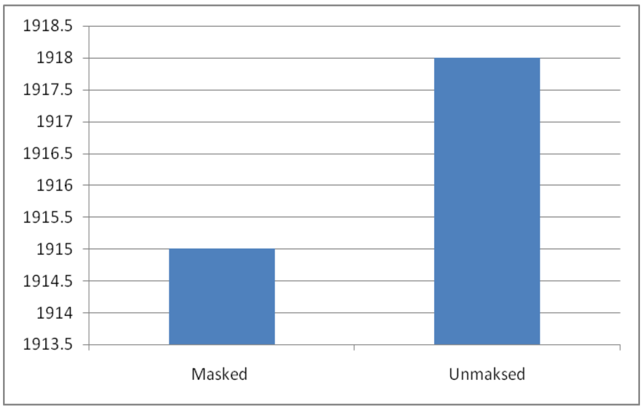

Figure 4: Total count of Masked vs. Unmasked records in the dataset

In this study, the seven extracted texture features using GLCM on (distances, angles) format are as follows (1, 0), (3, 0), (2, 0), (5, 0), and (5, π/2). The most often used value of every extracted characteristic is shown in Figure 5. The representation of the co-occurrence matrix utilizing color- coding is shown in (Figure 6) as a heat map of seven GLCM texture properties. A characteristic with a high degree ofcorrelation is represented by a light brown hue, whereas features with a low degree of co-relation are depicted by black color.

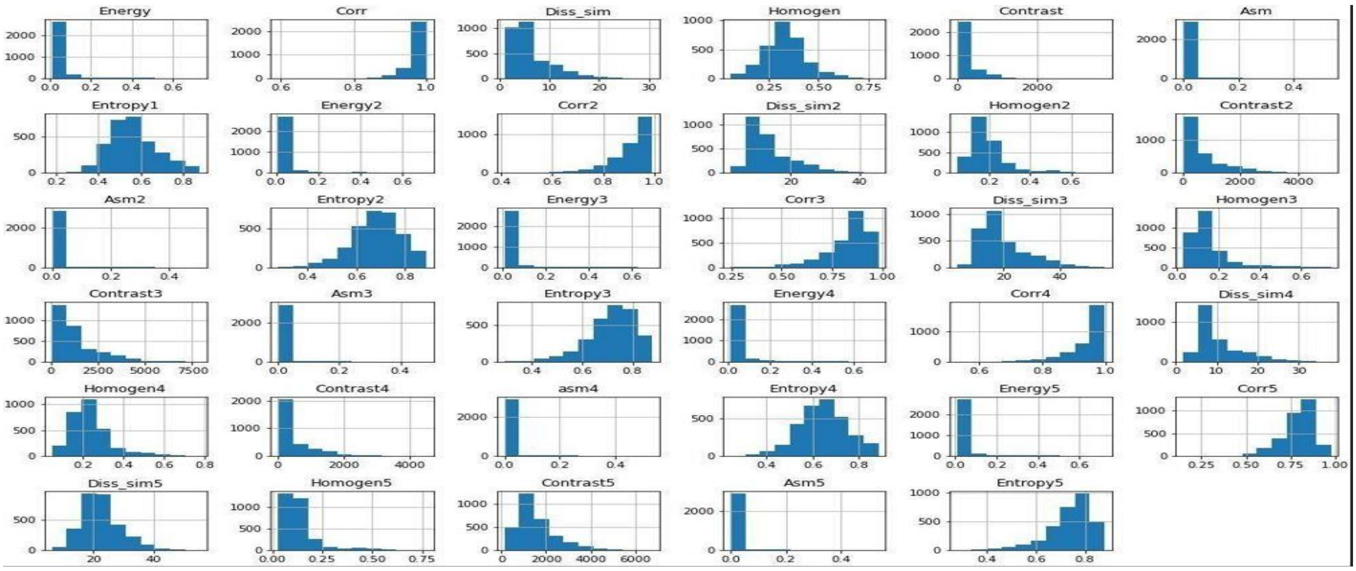

Figure 5: Value count of extracted characteristics

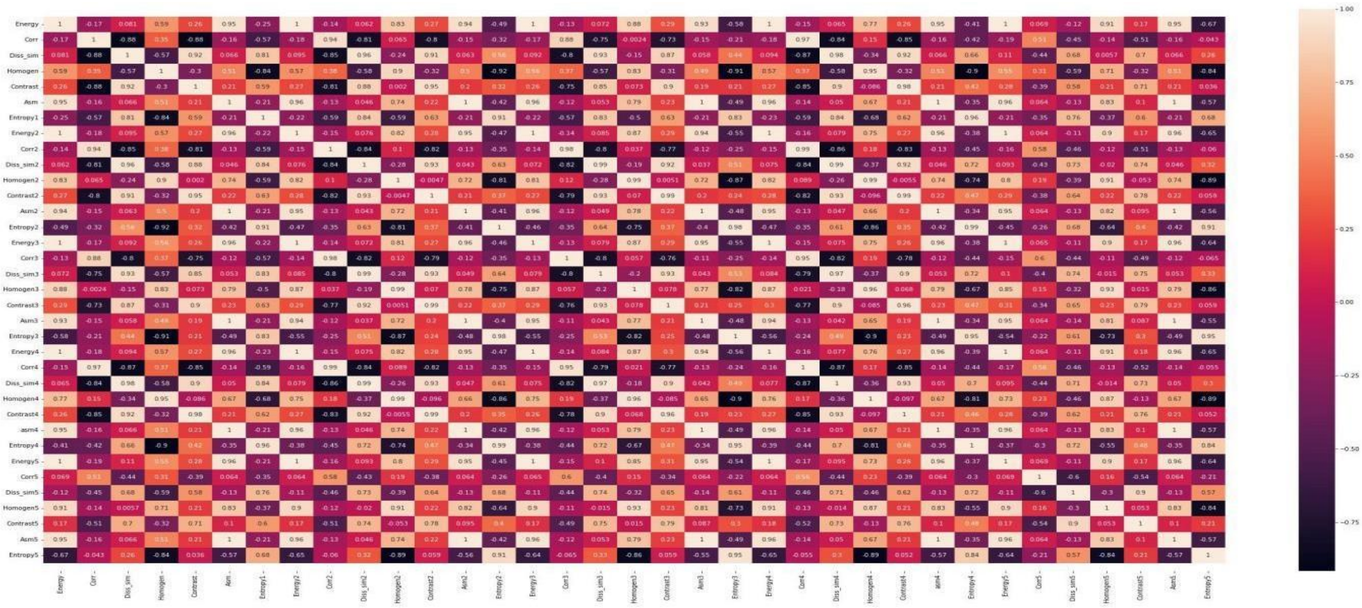

Figure 6: Heatmap of the extracted Texture Features

C. Classification Model

The extracted features are fed to LightGBM for classification; the output is compared to a threshold acquired from the AUC curve illustrated below. The concept of using the ROC curve for threshold adjustment consists in identifying the threshold that gives us the top left corner of the curve. In mathematical terms, that threshold p satisfies the equation (11)

$$TPR\ (p) = 1 - FPR\ (p)$$

In this study, the threshold was tuned to 0.445263

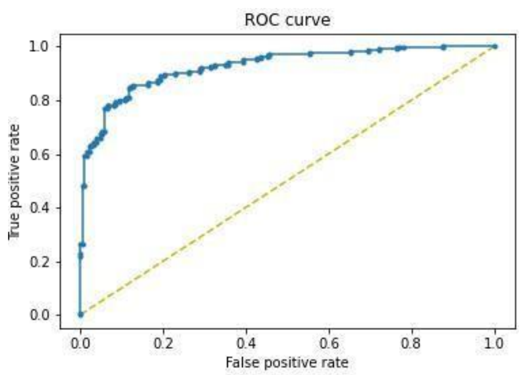

Figure 5: The suggested model's ROC curve, having an AUC of 0.93

LightGBM is a tree-based learning algorithm and gradient boosting paradigm created by Microsoft in 2016. With the following whip hand, engineered to all be distributed as well as effectual:

- Greater efficiency and a faster training pace.
- Reduced memory utilization.
- Superior accuracy.
- Distributed, Parallel, and GPU learning are all supported.
- Adept at dealing with massive amounts of data

Because of these capabilities, LightGBM is commonly found in various winning machine learning contest solutions.

On publicly available datasets, comparison trials [22] show that LightGBM outshines extant boosting frameworks in terms of efficiency and accuracy while consuming noticeably less memory. Furthermore, distributed learning studies [23] reveal that via leveraging many machines for training in precise conditions, LightGBM can obtain a linear speed-up.

D The learning rate for the LightGBM was fixed to 0.05, and the number of leaves was adjusted to 100 during the implementation of this proposed approach. The Tree plot of the LightGBM is shown in Figure 8.

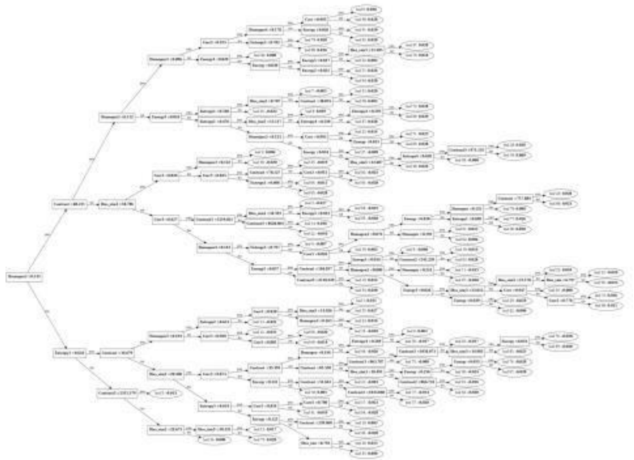

Figure 6: Tree plot of the implemented LightGBM

VI. METRICS FOR EVALUATING PERFORMANCE

To gauge the performance of the proposed approach, the highlighted metrics below were utilized. AP represents the correctly predicted unmasked individuals, FP is the masked individuals that were wrongfully classified as unmasked by the proposed model, and AN represents the masked cases that were suitably classified. At the same time, the FN denotes the unmasked cases that were misclassified as masked.

Accuracy = (AP + AN)/ (AN + FP + AP + FN)

Recall = AP/ (AP + FN)

Precision = AN/ (AN + FP)

F1 score = (AP × 2)/ (2 × AP + FP + FN)

Figure 9 below demonstrates the confusion Matrix acquired during the Testing phase of the proposed approach. There is a total of 54 misclassified images, 24 misclassified as unmask ed, and 30 images misclassified as masked. It is found that th e proposed approach provides an outstanding performance b ased on consistent actual positive and actual negative values and fewer false-negative and false-positive values. Hence, th e proposed system can efficiently detect masked individuals. Furthermore, Table 1 and Figure 10 show the performance m etrics of each class of the suggested approach. The accuracy i s 87% for masked cases and 85% for unmasked cases. The Pre cision is found at 85% and 88% for masked, Unmasked cases, respectively. The Recall is achieved at 87% for Masked and 8 6% for Unmasked cases. The f1-score is 86% for the masked c ases and 87% for the Unmasked class.

Table 1: Performance of the Suggested Method

Class	Accuracy	Precision	Recall	F1-Score
Masked	0.87	0.85	0.87	0.86
Unmasked	0.85	0.88	0.86	0.87

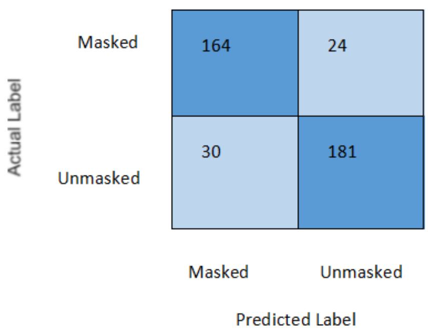

Figure 7: Confusion Matrix obtained during the test phase of the proposed approach

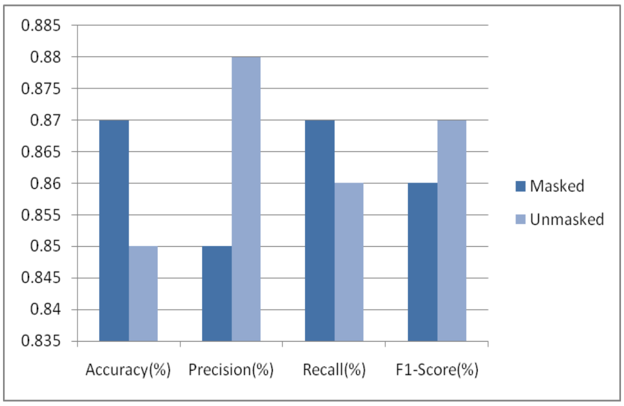

Figure 8: The graphical representation of the evaluation metrics results

VI. COMPARATIVE STUDY

The results indicate that using a combination of GLCM for fea ture extraction and LightGBM for recognizing masked individ uals based on the auto extraction of features from the input i mages has a substantial effect on detecting masked individua ls. The proposed approach could accurately discriminate bet ween masked and unmasked classes. Table 2 illustrates a co mparison of systems with our proposed GLCM-LightGBM syst em. Table 2 shows that the accuracy of some of the proposed methods [24], [25], and [26] was 97.3 percent, 96.5 percent, and 96.2 percent, respectively. The accuracy of most existing systems ranged from 80 % to 94 %, which is within the range of the proposed technique in this study.

Table 2: Comparative Table

Author	Architecture	Accuracy (%)
Rizki et al. [24]	CNN based Mode l	97.3
T.M. Saravanan e t al.[25]	Pre-trained Vgg1 6-based model	96.5
F.M. Javed M et a l. [26]	CNN-based mode l(Average pooling approach)	98.67%
F.M. Javed M et a l. [26]	CNN-based mode l(Max pooling ap proach)	96.23%
M.M. Rahman et al.[11]	CNN	98.7%
F.M. Javed M et a l. [26]	MobileNetV2	99.82%
Proposed approa ch	**GLCM-LightGBM**	**87%**

VII. CONCLUSION AND FUTURE SCOPE

GLCM Texture features were retrieved in this study, and Light GBM was employed to create a collaborative network for fac e mask detection. The fundamental goal was to develop a very accurate compatible model that would make mask detecti on straightforward, hence reducing the spread of airborne dis eases considering COVID19 as an example. The proposed mo del provided outstanding performance based on experimenta l results. Though the accuracy was not as high as some exist ing approaches, GLCM texture features still are compelling. T hey could be used in addition to other feature extraction mec hanisms like the Gabor filters for better results.

REFERENCES

[1] L. G. Goh, T. Ho, K. H. Phua, Wisdom and western science: The work of Dr. Wu Lien-Teh. Asia Pac. J. Publ. Health 1, 99– 109 (1987).

[2] L. T. Wu, A Treatise on Pneumonic Plague (League of Nations, Health Organization, 1926), pp. 373–398.

[3] Hollingsworth TD, Klinkenberg D, Heesterbeek H, Anderson RM. Mitigation strategies for pandemic influenza A:balancing conflicting policy objectives. PLoS Comput Biol2011;7:e1001076-76.doi:10.1371/journal.pcbi.1001076.pmid:21347316CrossRef PubMed Google Scholar

[4] C. T. Leffler et al., Association of country-wide coronavirus mortality with demographics, testing, lockdowns, and public wearing of masks. Am. J. Trop. Med. Hyg. 103, 2400–2411 (2020).

[5] C. Kenyon, Widespread use of face masks in public may slow the spread of SARSCoV-2:An ecological study. https://doi.org/10.1101/2020.03.31.20048652 (6 April 2020).

[6] J. Won Sonn and J. K. Lee, “The smart city as a time-space cartographer in COVID-19 control: the South Korean strategy and democratic control of surveillance technology,” Eurasian Geogr. Econ., pp. 1–11, May. 2020.

[7] Ge et al. [110] proposed an LLE-CNN to detect masked faces by combining pre-trained CNNs to extract candidate facial regions and represent them with high dimensional descriptors.

[8] Fan, X.; Jiang, M.; Yan, H. A Deep Learning-Based Lightweight Face Mask Detector with Residual Context Attention and Gaussian Heatmap to Fight against COVID-19. IEEE Access 2021, 9, 96964–96974. [CrossRef]

[9] M.S. Ejaz, M.R. Islam, M. Sifatullah and A. Sarker, "Implementation of principal component analysis on masked and non-masked face recognition," 2019 1st International Conference on Advances in Science Engineering and Robotics Technology (ICASERT), pp. 15, 2019.

[10] 10. Loey M, Manogaran G, Taha MHN, Khalifa NEM. A hybrid deep transfer learning model with machine learning methods for face mask detection in the era of the COVID-19 pandemic. Measurement: Journal of the International Measurement Confederation. 2021 Jan; 167:108288. DOI: 10.1016/j.measurement.2020.108288

[11] M. Jiang, X. Fan, and H. Yan, “RetinaMask: A Face Mask detector,” 2020. [Online]. Available: http://arxiv.org/abs/2005.03950.

[12] P. Ghosh, S. Azam, A. Karim, M. Jonkman, MDZ Hasan, “Use of Efficient Machine Learning Techniques in the Identification of Patients with Heart Diseases,” 5th ACM International Conference on Information System and Data Mining (ICISDM2021), 2021.

[13] M. S. Junayed, A. A. Jeny, S. T. Atik, N. Neehal, A. Karim, S. Azam, and B. Shanmugam, “AcneNet - A Deep CNN Based Classification Approach for Acne Classes,” 2019 12th International Conference on Information & Communication Technology and System (ICTS), 2019.
[14] A. Karim, P. Ghosh, A. A. Anjum, M. S. Junayed, Z. H. Md,K. M. Hasib, and A. N. Bin Emran, “A Comparative Study of Different Deep Learning Model for Recognition of Handwriting Digits,” SSRN Electronic Journal, 2021.
[15] Chen, Joy Long Zong, and S. Smys. Social Multimedia Security and Suspicious Activity Detection in SDN using Hybrid Deep Learning Technique. Journal of Information Technology 2, no. 02 (2020): 108-115.
[16] Smys, S., Joy Iong Zong Chen, and Subarna Shakya. Survey on Neural Network Architectures with Deep Learning. Journal of Soft Computing Paradigm (JSCP) 2, no. 03 (2020): 186-194
[17] K. shanmuga. Haralick, Robert M., “HaralickShanmugamDinstein1973.” 1973
[18] H. Y. Chai, L. K. Wee, T. T. Swee, S. Salleh, and a K. Ariff, “Gray-Level Cooccurrence Matrix Bone Fracture Detection Center for Biomedical Engineering Biomedical Engineering Group,” vol. 8, no. 1, pp. 26–32, 2011.
[19] J. Ding, X.-H. Hu, and V. Gudivada, “A Machine Learning- Based Framework for Verification and Validation of Massive Scale Image Data,” IEEE Trans. Big Data, vol. 7790, no. c, pp. 1–1, 2017.
[20] Z. Xing and H. Jia, “Multilevel Color Image Segmentation Based on GLCM and Improved Salp Swarm Algorithm,” IEEE Access, vol. 7, pp. 37672– 37690, 2019.
[21] Ambareen, Khateeja, et al. “Astrocytoma Type of Brain Tumor Classification Using Artificial Neural Network.” International Journal of Electronics Communication and Computer Engineering, vol. 5, no. 2, International Journal of Electronics Communication and Computer Engineering (IJECCE), Mar. 2014, p. 421a.
[22] Microsoft Corporation GitHub repository,https://github.com/microsoft/LightGBM/blob/master/docs/Experiments.rst#comparison-experiment
[23] Microsoft Corporation GitHub repository,https://github.com/microsoft/LightGBM/blob/master/docs/Experiments.rst#parallel-experiment
[24] 24. R. P. Sidik and E. Contessa Djamal, "Face Mask Detection using Convolutional Neural Network," 2021 4th International Conference of Computer and Informatics Engineering (IC2IE), 2021, pp. 85-89, DOI: 10.1109/IC2IE53219.2021.9649065
[25] Saravanan, T M et al. “A novel machine learning scheme for face mask detection using pre-trained convolutional neural network.” Materials today. Proceedings, 10.1016/j.matpr.2022.01.165. 21 Jan. 2022, doi:10.1016/j.matpr.2022.01.165
[26] F. M. J. Mehedi Shamrat, S. Chakraborty, M. M. Billah, M.A. Jubair, M. S. Islam and R. Ranjan, "Face Mask Detection using Convolutional Neural Network (CNN) to reduce the spread of Covid-19," 2021 5th International Conference on Trends in Electronics and Informatics (ICOEI), 2021, pp. 1231- 1237, DOI: 10.1109/ICOEI51242.2021.9452836.